JOURNAL OF MATERIALS SCIENCE 26 (1991) 4588–4598

Morphological changes of electrodeposited Zn and Zn–Fe coatings during heating

M. GU, A. R. MARDER
Energy Research Center, Lehigh University, Bethlehem, PA 18015, USA

The planar surface morphology of as-plated Zn crystals was found to be plate-like with a highly preferred orientation, whereas, the Zn–Fe coatings showed a nodular morphology. These nodules were clusters of many small polyhedral crystals. The surface morphology of Zn and Zn–Fe coatings did not change on heating up to a critical temperature. On heating above that temperature the surface started to smear. This critical temperature was found to increase with average Fe content in the coating. The cross-sectional view of as-plated Zn–Fe coatings showed a banded structure where the average grain size of each band was determined to be about 30 nm. As heat treatment progressed, the bands gradually disappeared. The pure Zn coating formed a layered structure with each layer corresponding to a different phase.

1. Introduction

The surface morphology of Zn and Zn–Fe coatings is very important to their deformation characteristics, paint adhesion, and corrosion resistance [1–4]. It is, therefore, very important to define the surface morphology and its variation during heating. Previous studies showed that the morphology of the coatings is dependent on the Fe content in the coating. The pure Zn deposits are plate-like in appearance [4–6]. Takechi [5] and Ohmori *et al.* [6] reported that Zn deposits nucleated on a steel surface have the orientation relationships with the ferrite grain: $(0\,0\,0\,1)_{Zn}||(1\,1\,0)_{\alpha}$ and $[\bar{2}\,1\,1\,0]_{Zn}||[\bar{1}\,1\,1]_{\alpha}$. In commercial deposits, however, the pyramidal planes $(1\,0\,\bar{1}\,1$, $1\,0\,\bar{1}\,2$, ... $1\,0\,\bar{1}\,X)$ are oriented parallel to the steel substrate [4]. As the Fe content in the coating increases, the deposited crystals change successively from plates to fine and sharp-edged polyhedra, to round-edged polyhedra and finally to granular crystals [6, 7].

In addition to Fe content, impurities, current density, variations of potential, and hydrodynamics of the catholyte flow, etc., all have a significant effect on the morphology of the coating [8]. The effect of heat treatment, however, on the morphology of electrodeposited Zn and Zn–Fe coatings has not been reported in the literature. The aim of the present work was to examine this effect. The techniques used in the study were light optical microscopy (LOM), scanning electron microscopy (SEM), electron probe microanalysis (EPMA), transmission electron microscopy (TEM), and X-ray diffraction (XRD).

2. Experimental procedure

The materials used in this study were all commercially produced. The electrogalvanized coating (EG), about 7 μm thick, was deposited on a cold-rolled steel substrate. The electrodeposited Zn–Fe (EZF) alloy coatings are of two compositions, one with 11 wt % Fe (LA), the other with 18 wt % Fe (HF). These coatings were 8 μm thick and were also deposited on a cold-rolled steel substrate about 0.7 mm thick. The chemical compositions of the steel substrate determined from spectrochemical analysis, are shown in Table I.

The LOM and EPMA specimens were cut as 18 mm × 14 mm pieces using a shear. Each specimen was mounted in a bakelite ring filled with epoxy resin. In order to avoid rounding of the edges and gas-bubble absorption on the coating surface, four additional pieces of steel sheet, of the same size were mounted on each side of the specimen. They were separated by spacers that were 0.1 mm thick, as shown schematically in Fig. 1. Two steel bars were placed in the mount for better maintenance of orthogonality between the flat and the circular cylindrical surfaces when grinding. To mount the specimen, epoxy resin was first poured to about half the height of the ring. The specimen was then placed in an evacuated chamber to draw out gas bubbles from the epoxy resin. The epoxy resin was then poured to full height and cured at room temperature for 5 days. The specimen was successively ground with silica papers of numbers 240,

TABLE I Chemical compositions of steel substrate (wt %)

Element	Sample EG	Sample LA	Sample HF
C	0.043	0.037	0.044
Mn	0.21	0.22	0.22
P	0.012	0.010	0.012
S	0.010	0.014	0.014
Si	0.01	0.01	0.03
Ni	0.02	0.05	0.04
Cr	0.06	0.08	0.08
V	< 0.001	< 0.001	< 0.001
Cu	< 0.001	0.068	0.052
Al	0.085	0.082	0.080
Fe	99.5	99.36	99.36

0022–2461/91 $03.00 + .12

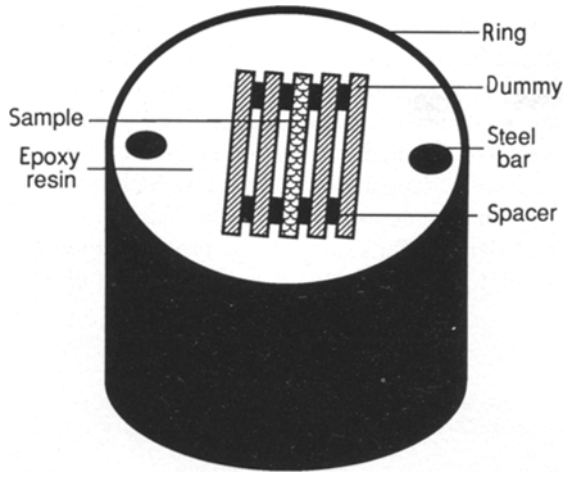

Figure 1 Configuration of cross-sectional samples used for LOM and EPMA.

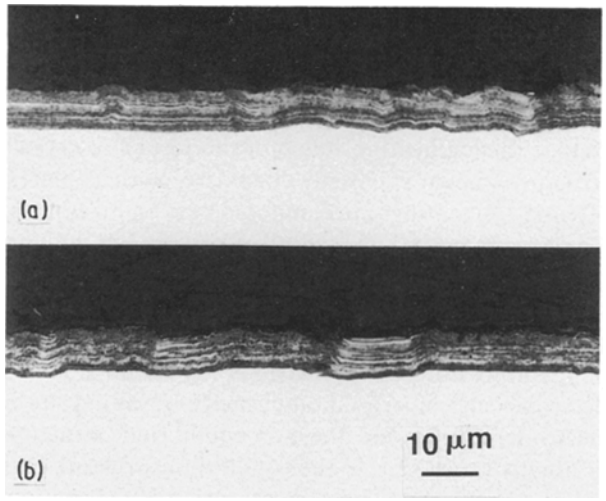

Figure 2 Light optical micrographs showing the band structure for as-plated (a) HF coating, and (b) LA coating. Etchant: Rowland no. 4 [9].

320, 400 and 600, 8, 3 and 1 μm, and polished with 1 μm and $\frac{1}{4}$ μm diamond pastes. Roland etchant number 4 [9] was used for LOM specimens of the EZF coatings. Instead of etching, an evaporated carbon film several tens of nanometres thick was deposited on the polished surface for EPMA specimens. The LOM observation was performed on a Zeiss light optical microscope. The EPMA was carried out on a Jeol 733 Superprobe equipped with an energy dispersive and three-wave dispersive spectrometers. The SEM observation was carried out on an ETEC Autoscan SEM with an energy dispersive spectrometer.

Transmission electron microscopy was used to determine the cross-sectional morphology of the coatings. The preparation of TEM specimens has been described elsewhere [10]. The TEM observations were carried out on a Philips 400 transmission electron microscope with an energy dispersive spectrometer operated at an acceleration voltage of 120 kV.

The XRD experiments were performed using a Philips XRG3100 X-ray generator with an APD3720 Automated Diffractometer System. CuK_α radiation was used at 45 kV and 30 mA. A computer program of "Profile Fitting", supplied by the Philips company, was used to obtain integrated peak intensity. The quantitative analysis from the measured integrated peak intensities was performed by an iterative external standard method, which is described elsewhere [11].

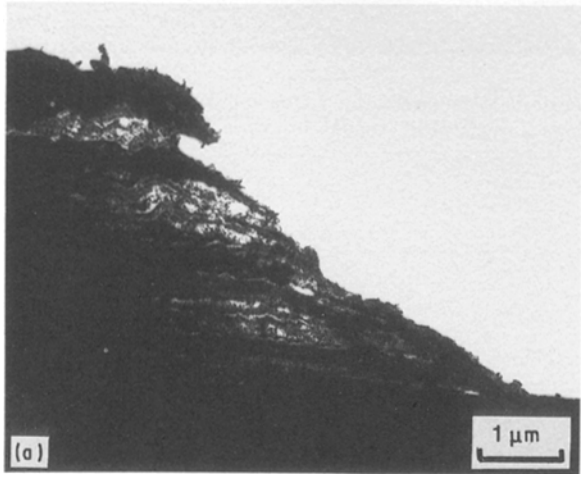

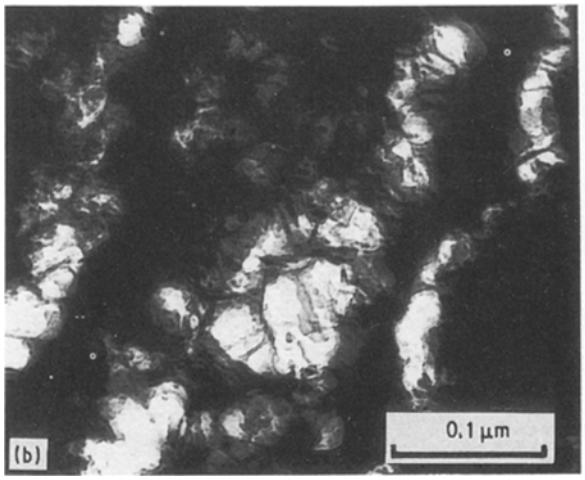

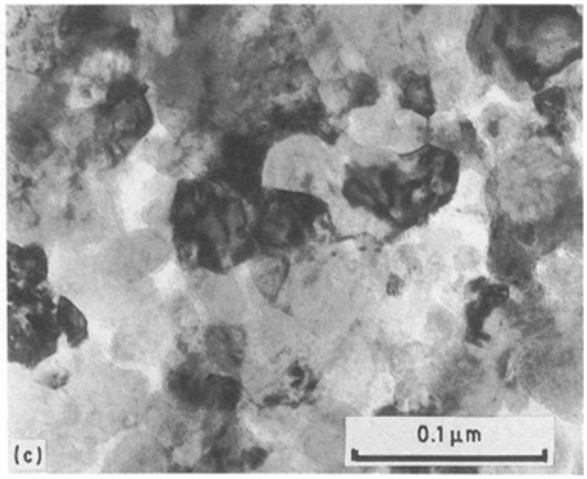

Figure 3 Transmission electron micrograph of as-plated HF coating showing (a) a large number of bands in the coating, (b) a band at high magnification, (c) the grains within a band. The average grain size is about 0.03 μm.

3. Results and discussion

The variation of the crystal structure of HF and LA coatings during heating is described elsewhere [10]. For a better understanding of the morphological change during heating, some of the results of crystal structure change are briefly cited here. Both as-plated HF and LA coatings are composed of δ- and η-phases. There is 88.2 ± 5.3 wt % δ-phase in the HF coating and 79.1 ± 4.7 wt % δ-phase in the LA coating. The transformations of EZF coatings during heating can be described by two temperature ranges. In the low-temperature range, interdiffusion between small grains decreases the micro-inhomogeneity resulting from electrodeposition and the non-equilibrium structure gradually transforms to the equilibrium structure corresponding to the average composition of the coating. For the HF coating, the η-phase transforms to δ-phase, and the δ-phase transforms to Γ_1-phase, and for the LA coating, the η-phase transforms to δ-phase. In the high-temperature range, the diffusion between the coating and the substrate is the dominant process. The iron content in the coating increased rapidly and new phases formed between the coating and the substrate. For the detailed information, the reader is referred to [10].

The cross-sectional light optical micrographs in Fig. 2 show a similar banded structure for both as-plated HF and LA coatings. A similar structure was observed in electrodeposited Zn–Ni [12] and Ni–Co [13] alloy coatings, and the band width was reported to increase with deposition temperature and current density [12]. The microstructural detail within the bands cannot be seen from these micrographs due to the resolution limit of the light optical microscope. The high-magnification transmission electron micrographs in Fig. 3, reveal additional sub-bands within the band structure of the coating and small grains are clustered within each band whose width is about 0.2–0.3 μm. The average grain size is about 0.03 μm which was measured from several TEM bright-field images. The banded structure may result from small variations in deposition parameters, such as current density in the deposition process. Variation of the current density, for example, can produce small compositional gradients between adjacent rows of grains

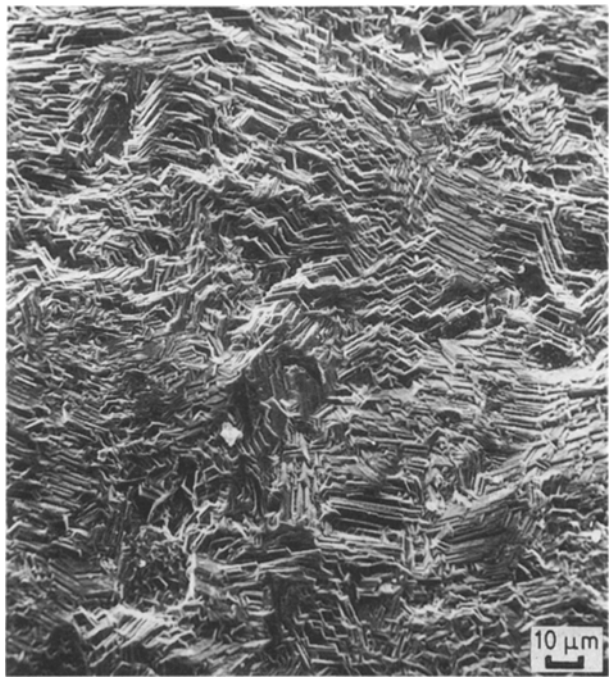

Figure 4 Scanning electron micrograph shows the surface morphology of as-plated EG coating.

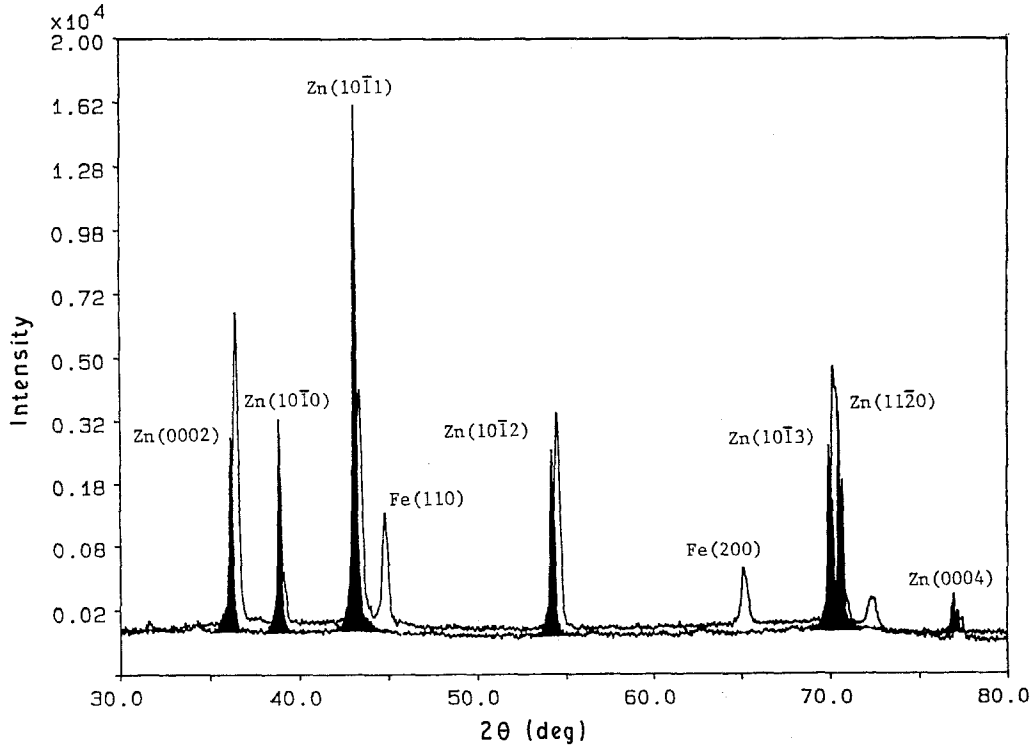

Figure 5 X-ray diffraction patterns for EG coated steel sheet (unfilled pattern), and pure zinc powder (filled pattern).

[14]. The composition differences between adjacent grains were not measured because the grain size was too small.

The scanning electron micrograph of Fig. 4 shows the surface morphology of an EG coating to be platelike. The preferred crystallographic orientation of the zinc coating was analysed with an inverse pole figure method [15–17]. The X-ray diffraction patterns of an EG coating as well as pure Zn powder are shown in Fig. 5. To assess the preferred orientation, the measured integrated peak intensity from each peak of the EG coating is divided by the intensity from corresponding peaks of the pure Zn powder. The sum of each obtained intensity ratio is divided by the number of peaks to get an average peak intensity ratio. Each peak intensity ratio is then divided by the average intensity ratio to get an orientation factor for each peak. If the orientation factor for a specific peak is larger than 1, it indicates that the planes of that peak prefer to orient themselves parallel to the coating surface. The larger the orientation factor, the stronger the preference. The measured and calculated data are shown in Table II. The bar graph in Fig. 6 indicates that the prominent plane parallel to the coating surface is the $(10\bar{1}3)$. The next prominent plane is the (0002), followed by $(10\bar{1}2)$. All other planes have intensities below average. It can be seen from Fig. 4 that the morphology of the Zn deposits changed markedly from one region to another. Kamei and Ohmori [18] have shown that these regions correspond to grains of the ferrite substrate, and the interfaces separating regions of the same orientation correspond to the grain boundaries of the substrate.

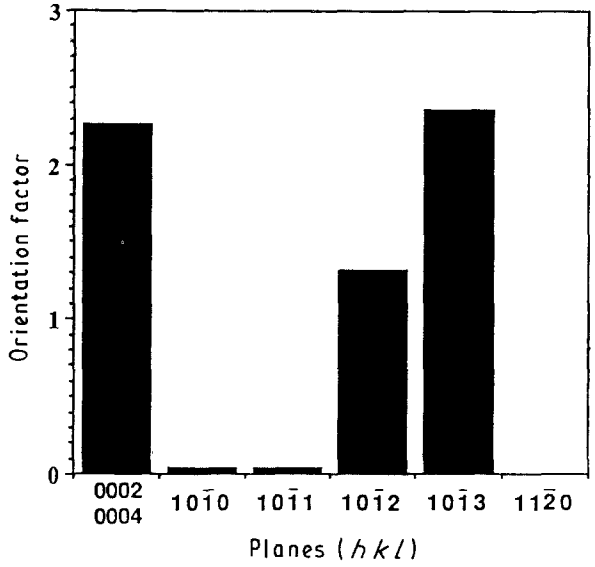

Figure 6 Bar-graph of the inverse-pole figure data for an EG coating shows the tabulation of the data for the plane parallel to the coating surface: major plane is $(10\bar{1}3)$.

TABLE II Inverse pole figure data sheet

hkil	I_{Zn}	I_{EG}	I_{EG}/I_{Zn}	Orientation ratio
0002, 0004	16266	50822	3.124	2.26
$10\bar{1}0$	14611	747	0.051	0.04
$10\bar{1}1$	76378	2890	0.038	0.03
$10\bar{1}2$	9938	18171	1.828	1.32
$10\bar{1}3$	9782	31935	3.265	2.36
$11\bar{2}0$	12582	0	0	0

Fig. 7 shows the nodular surface morphology of as-plated HF and LA coatings, respectively. The nodules are clusters of many smaller polyhedral crystals.

Light optical micrographs of the HF coating, after continuous heating at the rate of 10 °C min^{-1}, are shown in Fig. 8. At lower heating temperatures, the coating morphology changed very little, because only short-range diffusion took place. The composition profiles after heating to 270 °C, determined by EPMA,

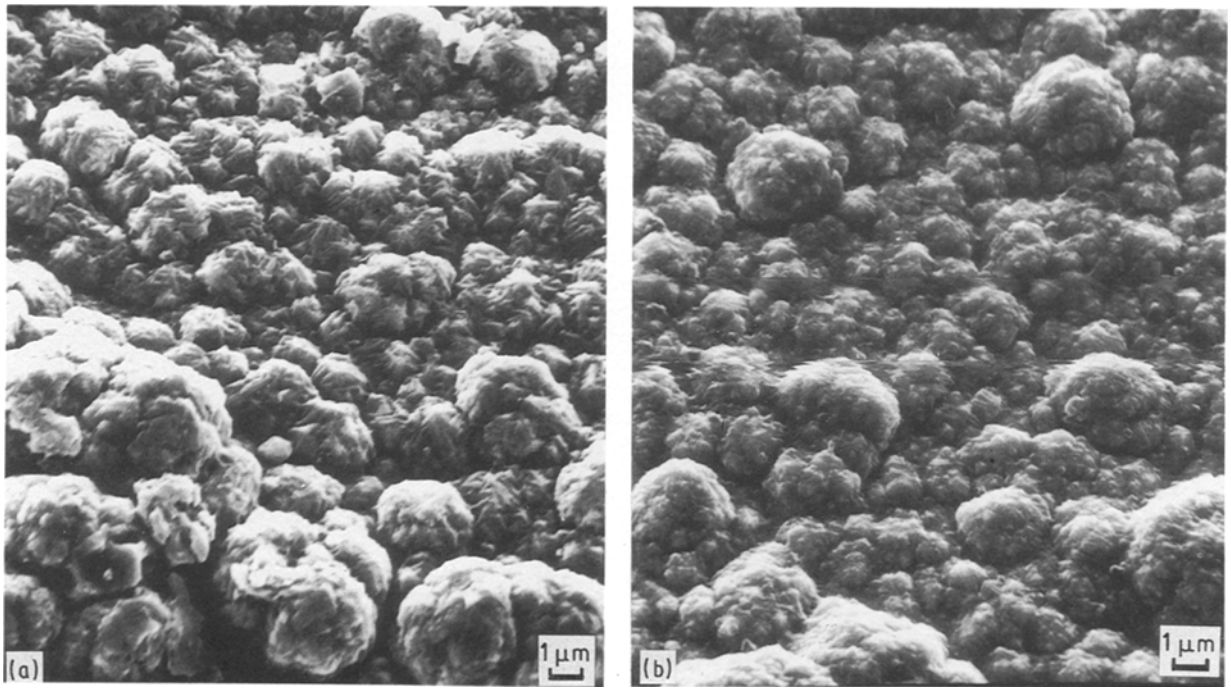

Figure 7 Scanning electron micrographs showing the surface morphology of as-plated (a) HF; (b) LA coatings.

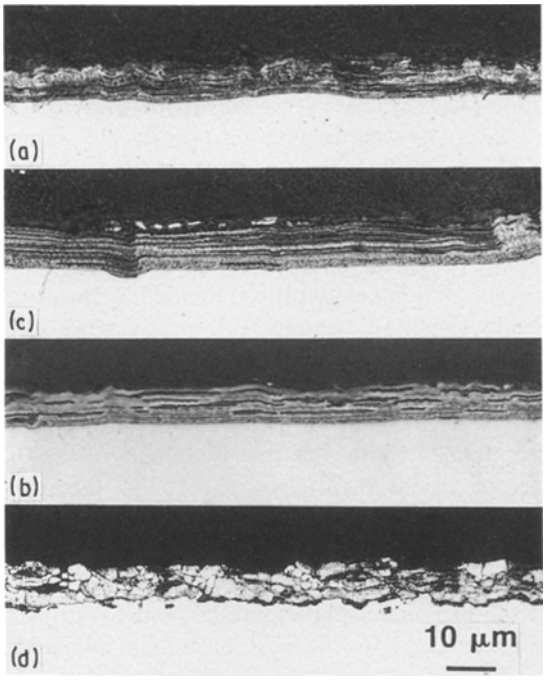

Figure 8 Light optical micrographs of an HF coating during continuous heating: (a) as-plated, (b) heated to 270 °C, (c) heated to 400 °C, (d) heated to 550 °C (heating rate 10 °C min^{-1}).

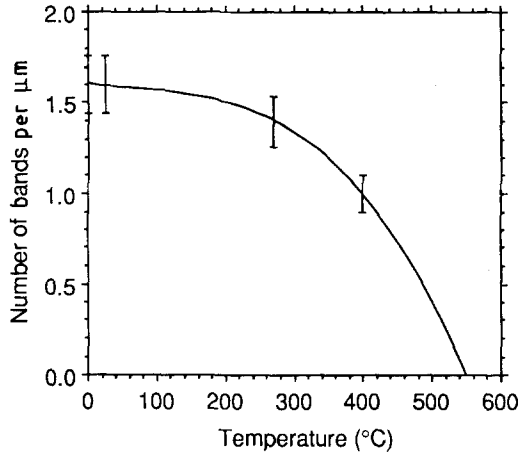

Figure 10 Variation in the number of bands distinguishable in LOM with continuous heating temperature of HF coating (heating rate 10 °C min^{-1}).

shown in Fig. 9c and d, are very similar to those of the as-plated coatings, shown in Fig. 9a and b. As the temperature increased, the compositional inhomogeneity decreased and the number of bands in the coating decreased. This variation in the average number of bands with temperature is illustrated in Fig. 10. The datum "0" at 550 °C illustrates that the banded structure has totally been replaced by a grain structure. During isothermal heating, when the specimen was heated at low temperature for a short time, the banded structure did not change much. At high temperature, however, the number of bands diminished quickly, and a new layer of Γ-phase formed and grew between the original coating and the steel substrate (Fig. 11).

The EG coating, after heating, has a layered structure, as opposed to a band structure, with each layer corresponding to a different phase. Two layers are shown in the light optical micrograph of an EG specimen, after heating to 300 °C for 16 h (Fig. 12a). The thin layer, near the steel substrate, is the Γ_1-phase, while the top, thick layer is δ-phase. This was proved

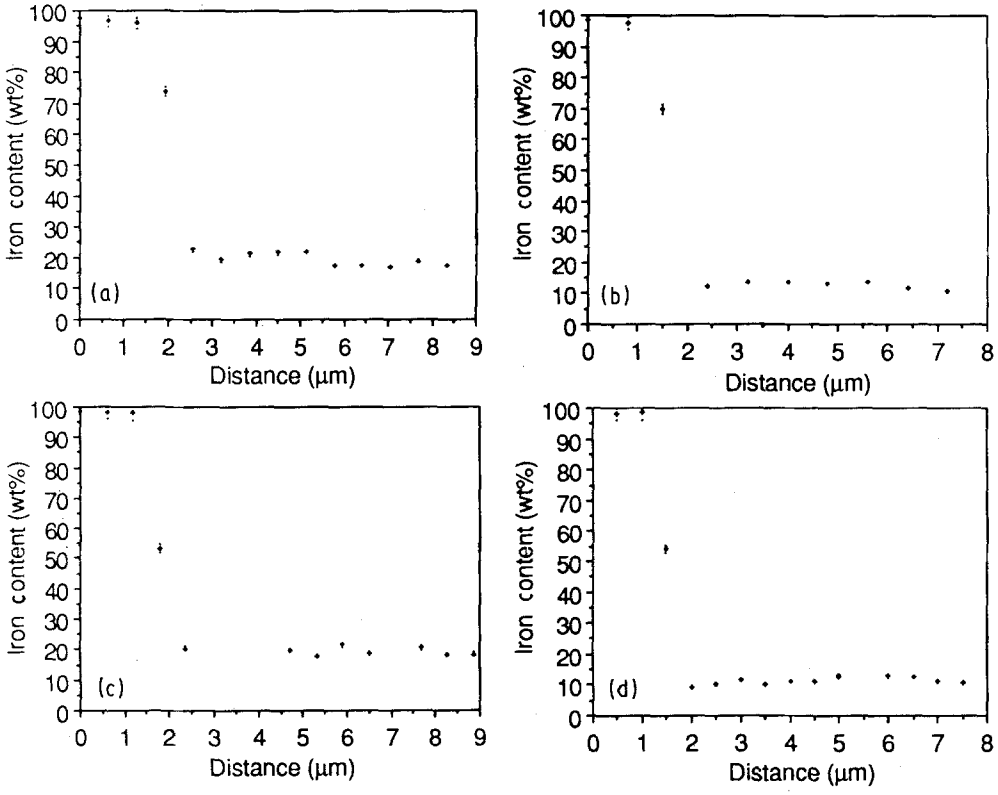

Figure 9 EPMA composition profiles of coatings: (a) as-plated HF coating, (b) as-plated LA coating, (c) HF coating after continuous heating to 270 °C (heating rate 10 °C min^{-1}), (d) LA coating after continuous heating to 270 °C (heating rate 10 °C min^{-1}).

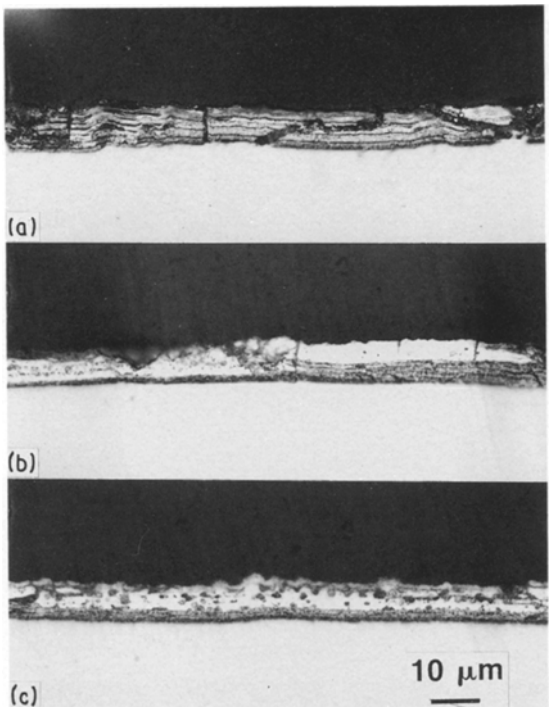

Figure 11 Light optical micrographs of an HF coating after isothermal heating at 400 °C for (a) 20 min, (b) 1 h, (c) 16 h.

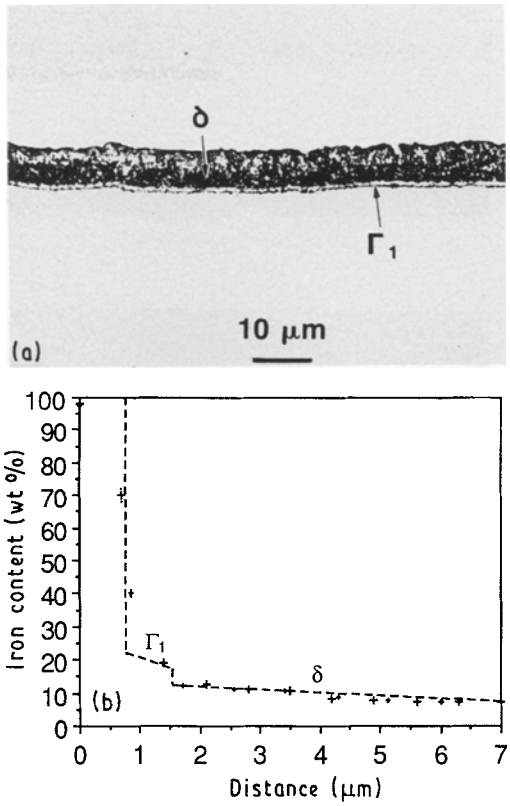

Figure 12 (a) Light optical micrograph showing the two layer structure, (b) EPMA composition profile, of an EG coating after heating at 300 °C for 16 h.

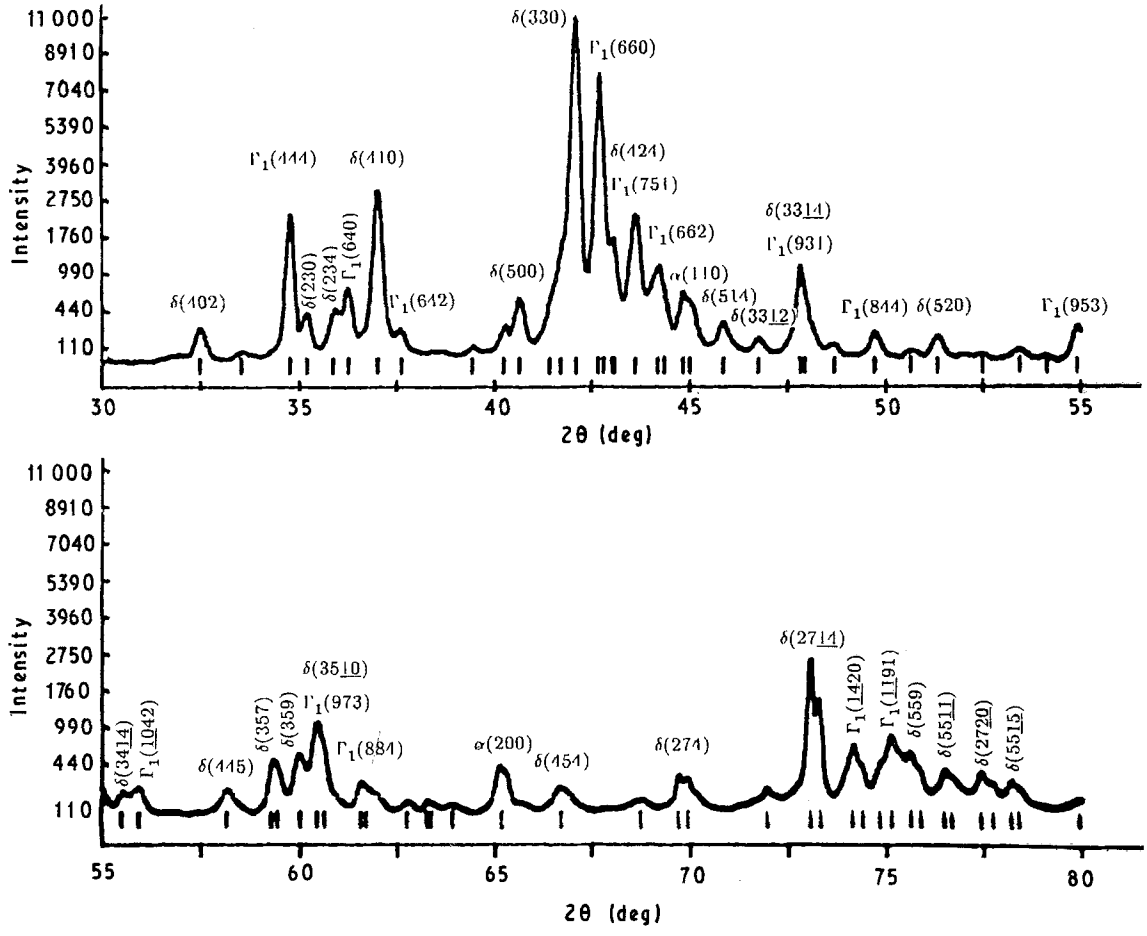

Figure 13 X-ray diffraction pattern of an EG coating after heating at 300 °C for 16 h.

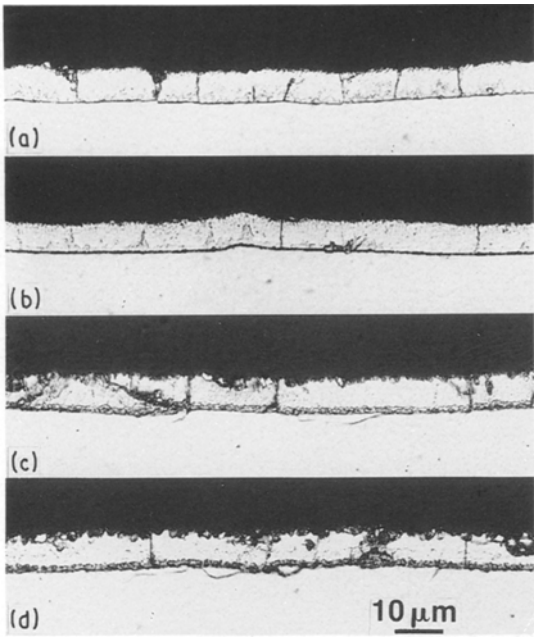

Figure 14 Light optical micrographs of an EG coating after heating to 400 °C for (a) 2 min, (b) 20 min, (c) 1 h, (d) 16 h.

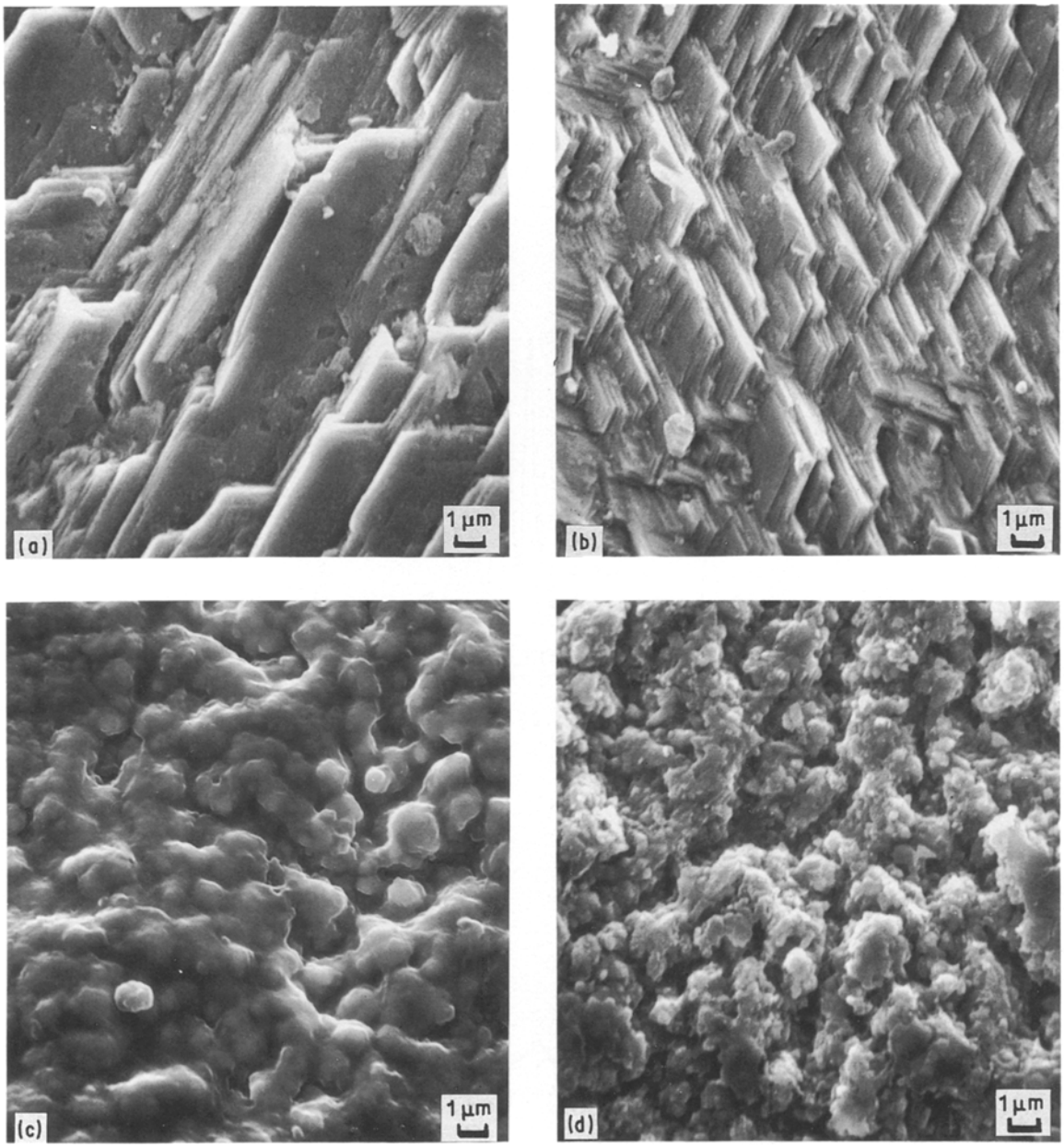

Figure 15 Scanning electron micrographs of an EG coating after heating to (a) 200 °C (10 °C min^{-1}), (b) 400 °C (10 °C min^{-1}), (c) 400 °C for 20 min, (d) 500 °C (10 °C min^{-1}).

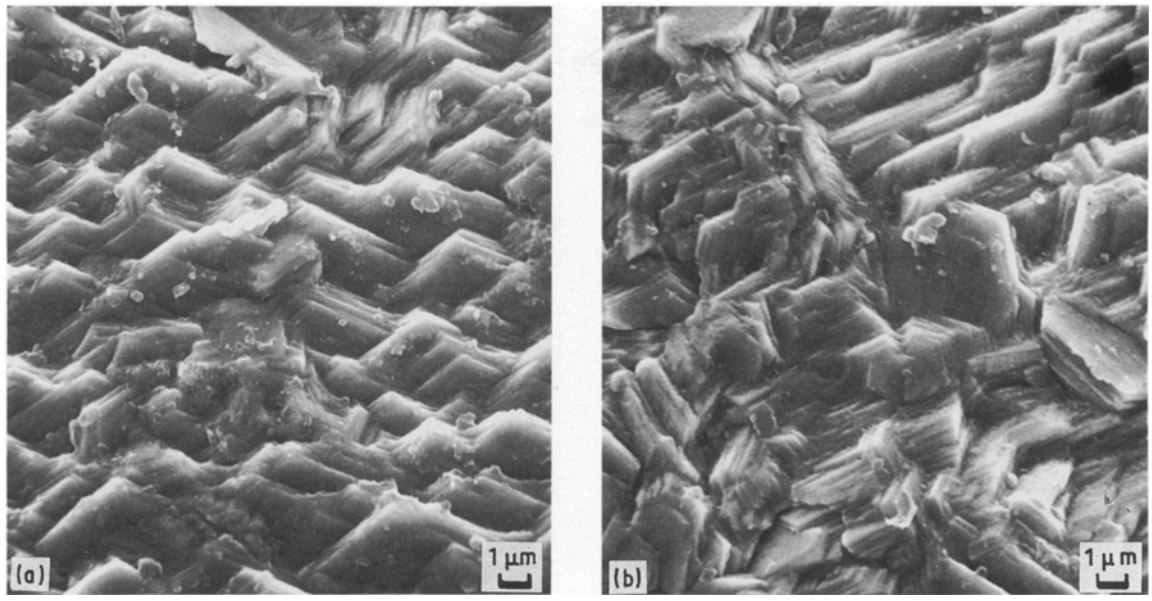

Figure 16 Scanning electron micrographs of an EG coating after holding for 16 h at (a) 100 °C, (b) 200 °C, (c) 300 °C.

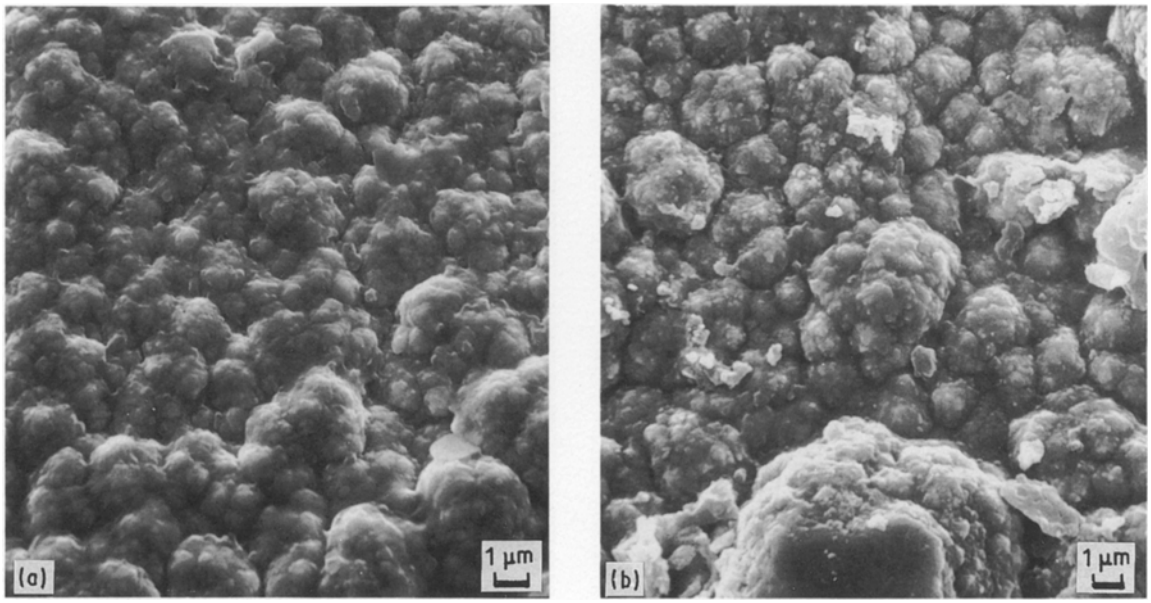

Figure 17 Scanning electron micrographs of an LA coating after heating to (a) 360 °C (10 °C min^{-1}), (b) 300 °C for 16 h, (c) 500 °C (10 °C min^{-1}), (d) 500 °C for 30 min.

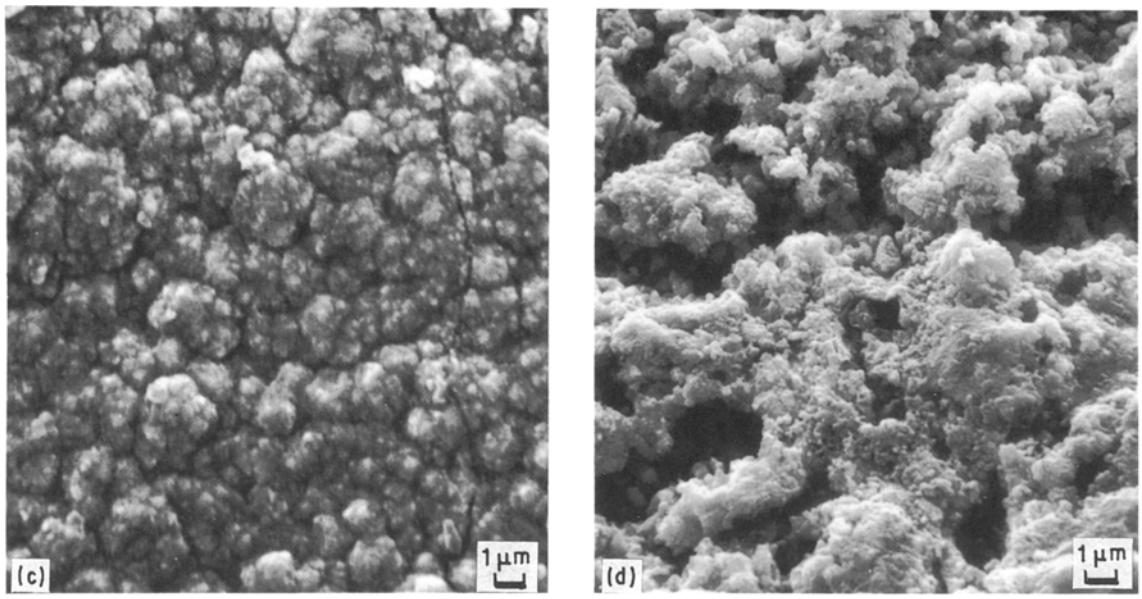

Figure 17 Continued

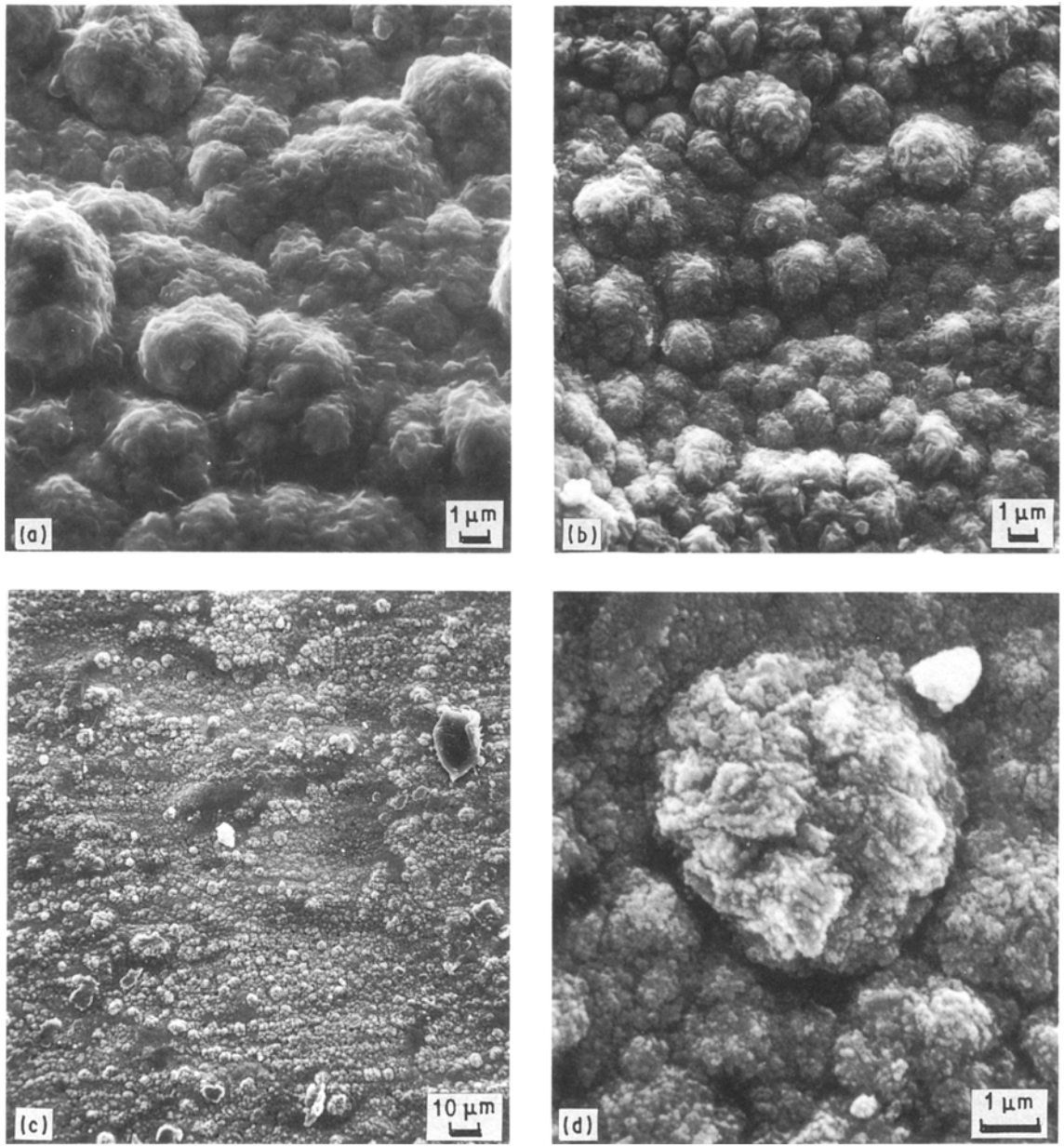

Figure 18 Scanning electron micrographs of an HF coating after heating to (a) 200 °C for 30 min, (b) 500 °C for 2 min, (c, d) 500 °C for 16 h.

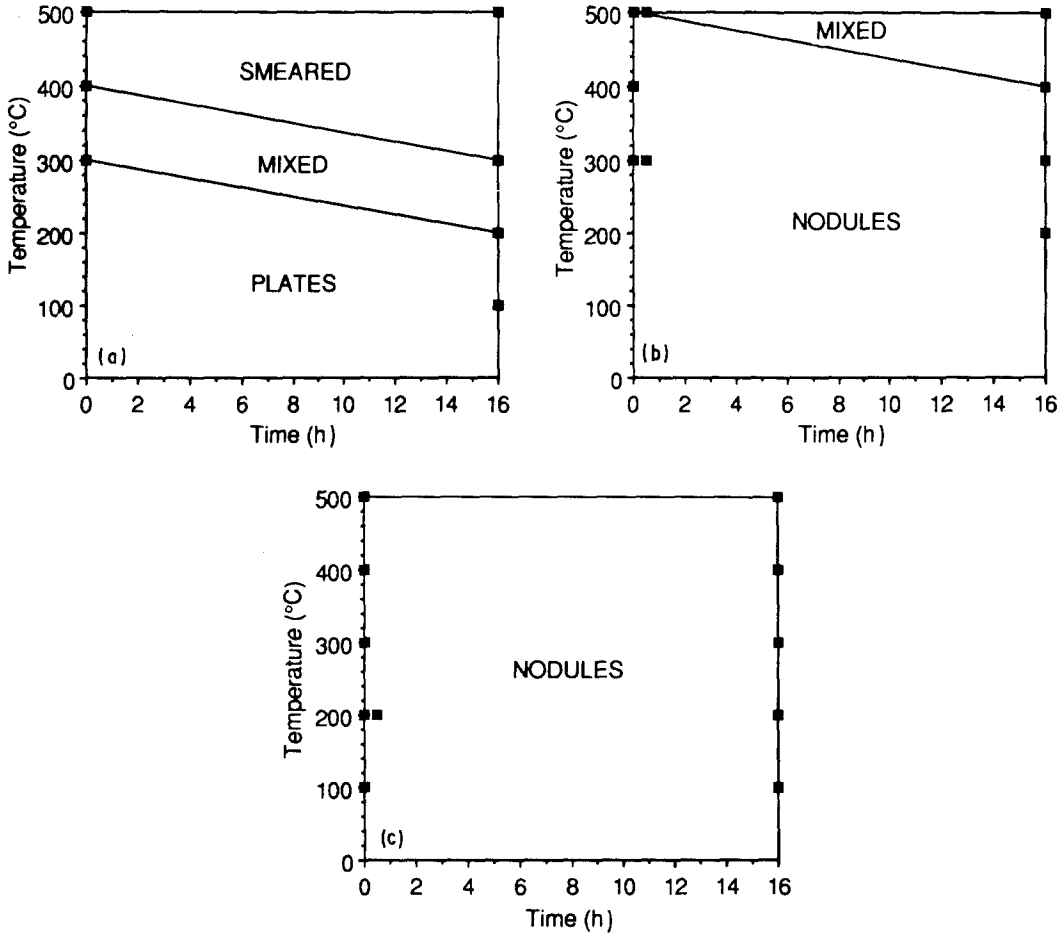

Figure 19 Effect of heat treatment on the surface morphology of (a) an EG coating, (b) an LA coating, (c) an HF coating.

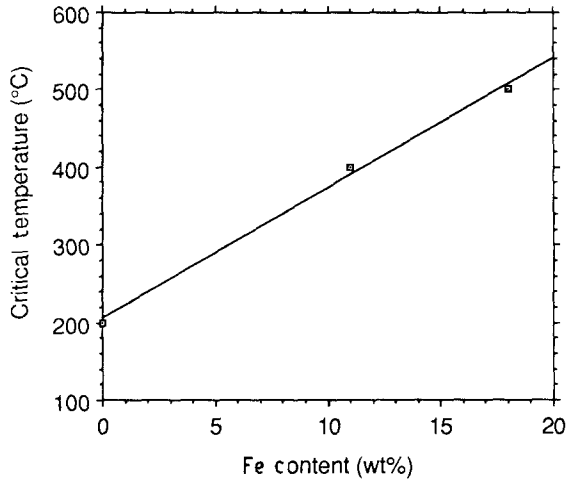

Figure 20 Effect of Fe content in as-plated coatings on critical temperature for a 16 h isothermal heating.

by EPMA compositional measurement (Fig. 12b), and XRD analysis (Fig. 13). The successive, morphological changes in the EG coating, after heating at 400 °C for different times are shown in Fig. 14.

Figs 15 and 16 show the changes in surface morphology of an EG coating after heating. During continuous heating at the rate of 10 °C min^{-1} to 400 °C, the plate-like morphology changed very little. However, when held at this temperature for some time (Fig. 15c), or continuously heated to a higher temperature (Fig. 15d), obvious changes in surface morphology were observed. During isothermal heating, the critical temperature, at which the surface morphology apparently changes, decreases with holding time. The longer the holding time, the lower the critical temperature. Fig. 16 illustrates that for a holding time of 16 h, the critical temperature of the EG coating was only about 300 °C. The same variation tendency in surface morphology is observed in the LA (Fig. 17) and HF (Fig. 18) coatings, except that the critical temperature for LA and HF increases with the Fe content in as-plated coatings. For the HF coating, the basic nodular feature of the surface morphology, and detailed structure in the nodule still remain after heating at 500 °C for 16 h, although the chemical composition and phase structure of the coating have changed during the heating process [10]. The above facts indicate that the surface morphology does not depend on phase structure, but does depend on the cumulative effects of diffusion. The above observations of the effect of heat treatment on surface morphology are summarized in Fig. 19. The effect of Fe content in as-plated coatings on the critical temperature is illustrated in Fig. 20 for a 16 h isothermal heating.

4. Conclusions

Based on the above experimental results and analyses, the following conclusions can be drawn about the structure and phase transformations during heating of electrodeposited Zn and Zn–Fe coatings.

1. The surface morphology of EG, LA, and HF coatings was observed in the scanning electron microscope. The zinc crystals in the EG coating are platelike. $(1\,0\,\bar{1}\,3)$ and $(0\,0\,0\,1)$ planes in these crystals prefer to orient themselves parallel to the coating surface. The surface morphology of LA and HF coatings are both nodular. The big nodules are composed of smaller nodules, which consist of many polyhedral crystals.

2. The surface morphology of EG, LA, and HF coatings does not change with temperature, up to a critical point. On heating above the critical temperature, the coating surface becomes smeared. The critical temperature increases with average Fe content in the coating.

3. The light optical microscopy examinations showed that the LA and HF coatings are composed of many bands. There are about 1.5 bands per micrometre distinguishable under the light optical microscope. The transmission electron microscopy examination indicated that one band, observed in the light optical microscope, is itself composed of several smaller bands with thicknesses of about 200–300 nm. The banded structure is proposed to be a result of compositional differences that arise from small fluctuations in the processing parameters, such as bath composition, and deposition current. The smaller bands are composed of grains with an average grain size of 30 nm, as shown by transmission electron microscopy.

4. The LOM cross-sectional examination showed that the bands in LA and HF coatings gradually diminished during heating. The EG coating, during heating, forms a layered structure, with each layer corresponding to a different phase. The ζ-phase is the first phase formed, followed by Γ-, δ-, and Γ_1-phase.

Acknowledgements

This work was supported by the International Lead Zinc Research Organization (ILZRO). The authors thank Dr Frank B. Goodwin, ILZRO, for helpful discussions.

References

1. H. LEIDHEISER Jr and D. K. KIM, *J. Metals* **28.11** (1976) 19.
2. D. JAFFREY, J. D. BROWNE and T. J. HOWARD, *Metall. Trans.* **11B** (1980) 631.
3. C. BELLEAU and D. K. KELLY, SAE Technical Paper Series, no. 840284 (1984).
4. J. H. LINDSAY, R. F. PALUCH, H. D. NINE, V. R. MILLER and T. J. O'KEEFE, *Plating and Surface Finishing* March (1989) 62.
5. H. TAKECHI, M. MATSUO, K. KAWASAKI and T. TAMURA, in "6th International Conference on Texture of Materials", Tokyo, September 1981 (Iron and Steel Institute of Japan, Tokyo, 1981) p. 43.
6. Y. OHMORI, K. KONDO, K. KAMEI and S. HINOTANI, *Mat. Res. Soc. Symp. Proc.* **122** (1988) 553.
7. T. HARA, T. ADANIYA, M. SAGIYAMA, T. HONMA, A. TONOUCHI, T. WATANABE and M. OHMURA, *Trans. ISIJ* **23** (1983) 954.
8. V. JIRICNY, H. CHOI and J. W. EVANS, *J. Appl. Electrochem.* **17** (1987) 91.
9. D. H. ROWLAND, *Trans. ASM* **40** (1948) 983.
10. M. GU, M. R. NOTIS and A. R. MARDER, in "Proceedings of the International Conference on Zinc and Zinc Alloy Coated Steel Sheet", Galvatech, '89 Keidanren Kaikan, Tokyo, Japan, 5–7 September 1989, pp. 462–77.
11. M. GU and A. R. MARDER, *Powder Diffraction*, **6**, No. 2 (1991).
12. B. LUSTMAN, *Trans. Electrochem. Soc.* **84** (1943) 363.
13. R. J. WALTER, *Plating and Surface Finishing* July (1980) 46.
14. C. DREWIEN, A. BENSCOTER and A. R. MARDER, *Mater. Charact.* **26** (1991) 45.
15. G. B. HARRIS, *Phil. Mag.* **43** (1952) 113.
16. M. H. MUELLER, W. P. CHERNOCK and P. A. BECK, *Trans. AIME* **212** (1958) 39.
17. B. L. BRAMFITT and M. H. LONGENBACH, *IMS Proc.* (1969) 45.
18. K. KAMEI and Y. OHMORI, *J. Appl. Electrochem.* **17** (1987) 821.

Received 11 April
and accepted 30 November 1990